Composites: Part A 92 (2017) 108–117

Contents lists available at ScienceDirect

Composites: Part A

journal homepage: www.elsevier.com/locate/compositesa

A probabilistic micromechanical modeling for electrical properties of nanocomposites with multi-walled carbon nanotube morphology

B.J. Yang [a], Ji-un Jang [a], Seung-Hyun Eem [b], Seong Yun Kim [a,*]

[a] Multifunctional Structural Composite Research Center, Institute of Advanced Composite Materials, Korea Institute of Science and Technology (KIST), 92 Chudong-ro, Bongdong-eup, Wanju-gun, Jeonbuk 55324, Republic of Korea

[b] Disaster Management HPC Technology Research Center, Korea Institute of Science and Technology Information (KISTI), 245 Daehak-ro, Yuseong-gu, Daejeon 34141, Republic of Korea

ARTICLE INFO

Article history:
Received 25 August 2016
Received in revised form 31 October 2016
Accepted 7 November 2016
Available online 9 November 2016

Keywords:
A. Polymer-matrix composites (PMCs)
A. Carbon nanotubes and nanofibers
B. Electrical properties
C. Micro-mechanics

ABSTRACT

The nanoscopic characteristics of the multi-walled carbon nanotubes (MWCNTs) used in composites are crucial for attempting to understand and design nanocomposites of a novel class. We investigate the correlations between the nanofiller properties and effective electrical properties of MWCNT-embedded polycarbonate composites by theoretical and experimental approaches. A probabilistic computational model is proposed to predict the influence of MWCNT morphology on the electrical behaviors of MWCNTs-embedded polymer composites. A parameter optimization method in accordance with a genetic algorithm is then applied to the model, resulting that the ideal sets of model constant for the simulation are computationally estimated. For the experimental validation purpose, a comparison between the present theoretical and experimental results is made to assess the capability of the proposed methods. In overall, good agreement between the predictions and experimental results can be observed and the electrical performance of the composites can be improved as the MWCNT length increases.

1. Introduction

Multi-walled carbon nanotubes (MWCNTs) have been utilized in a variety of composite applications as well as for reinforcements and nanofillers owing to their excellent mechanical, thermal, and electrical properties [1–3]. Specifically, the improved electrical characteristics of composites are expected to have a significant impact on numerous industrial applications [4], and therefore, the development of electric-related functionality has been actively researched in recent years [5,6]. However, the results of efforts to enhance the characteristics of composite materials can differ greatly depending on filler-matrix combinations and the fabrication methods used. Various studies which have attempted to optimize related variables have done thus far [5–9].

Polycarbonate (PC) has high toughness, exceptional impact resistance, and good dimensional stability as well as excellent optical clarity [7,8]. These outstanding properties of this PC resin make it a successful engineering thermoplastic which has been used in many engineering applications [8,9]. However, the utilization of PC-based polymers remains limited due to its insulating characteristics. Hence, electrical charge mitigation is a key factor which has been used to enhance the applicability of these polymers, offering protection from lightning and electromagnetic shielding. Although some studies [8,9] have addressed the electrical conductivity of PC composites filled with carbon nanotubes (CNTs), the relationship between the electrical conductivity and internal structure of the composites as analyzed based on non-destructive methods has not been clearly identified.

Hence, there has been a great interest in a theoretical method which can understand and analyzes electrical properties of nanoscale system. In general, atomistic modeling has been regarded as the most accurate approach [10,11]; however, the maximum simulation range being hundreds of nanometer made it challenging to generalize as a representative volume element of the nanocomposite [12]. Moreover, the atomistic modeling requires high levels of computational power, which makes it inaccessible without using a massive parallel supercomputer [13]. There was also a theoretical analysis of nanocomposites through classical microscopic method, but it was difficult to comprehend inherent characteristics in nanoscopic scale [14–16]. Hence, probabilistic modeling recently has grasped a keen interest as a new paramount research method to overcome these limitations. From this perspective, material properties that are difficult to obtain and generalize by experiments (e.g., interfacial resistivity, tunneling region, and filler waviness) would be determined probabilistically. A proper

* Corresponding author.
E-mail address: sykim82@kist.re.kr (S.Y. Kim).

http://dx.doi.org/10.1016/j.compositesa.2016.11.009
1359-835X/

derivation of probabilistic material modeling not only makes it capable to explain through concepts when some test results cannot be answered, but also helps to predict a scientific phenomenon based on an initial condition of system.

The objective of this study is to develop a rigorous but effective probabilistic model to predict the electrical property of MWCNT-embedded polymer composites. Herein, the relationship between the MWCNT characteristics and the effective electrical properties of MWCNT-embedded PC matrix composites is investigated by theoretical and experimental approaches. A probabilistic micromechanics-based model taking into account interfacial resistivity, tunneling effects, and morphological waviness of MWCNTs is developed for predictions of the electrical behaviors with different material constituents [17]. The optimal combination of model constants for this simulation is estimated by the computational method based genetic algorithm [18]. In addition, two types (30–130 μm for short and 150–250 μm for long) of MWCNTs are considered as a nanofiller material to enhance the electrical properties of composites, and the effects of the internal morphology and the characteristics of the MWCNTs on the nanocomposites are analyzed.

2. Theoretical modeling

Based on the effective medium theory [19,20], the electrical conductivity of three-dimensional (3D) randomly oriented and distributed MWCNT-reinforced composites can be estimated as [19,20]

$$\phi_0\left[(\mathbf{L}_0-\mathbf{L}_e)^{-1}+\mathbf{S}_0\mathbf{L}_e^{-1}\right]^{-1}+\phi_1\left[(\mathbf{L}_1-\mathbf{L}_e)^{-1}+\mathbf{S}_1\mathbf{L}_e^{-1}\right]^{-1}=0 \tag{1}$$

with

$$(S_{11})_1=(S_{22})_1=\begin{cases}\frac{\alpha}{2(1-\alpha^2)^{1.5}}\left[\cos^{-1}\alpha-\alpha(1-\alpha^2)^{0.5}\right], & \alpha<1\\ \frac{\alpha}{2(\alpha^2-1)^{1.5}}\left[\alpha(\alpha^2-1)^{0.5}-\cosh^{-1}\alpha\right], & \alpha>1\end{cases} \tag{2}$$

$$(S_{33})_1=1-2(S_{11})_1$$

where ϕ denotes the volume fraction of the MWCNTs; $\mathbf{L}$ signifies the conductivity tensor; $\mathbf{S}$ is the aspect ratio (α) dependent depolarization tensor, which the subscripts 0, 1 and e represent the material phase of the polymer, MWCNTs, and effective nanocomposite, respectively. The components of $\mathbf{S}_1$, taking 33-direction as the symmetric axis of the MWCNTs, is given in Eq. (2), while $\mathbf{S}_0$ is mathematically converged to 1/3 [19].

By using the Cauchy's probabilistic model, the effective electrical conductivity of nanocomposites considering interfacial resistivity due to a tunneling effect can be expressed as [19,20]

$$\sigma_{ii}^c=\frac{r\alpha\sigma_{ii}}{r\alpha+S_{ii}\sigma_{ii}(1+2\alpha)\rho(\phi_1)} \tag{3}$$

in which

$$\rho(\phi_1)=\frac{\rho_0\left[1-F(\phi_1;\phi_1^*,\gamma)\right]}{\left[1-F(0;\phi_1^*,\gamma)\right]} \tag{4}$$

with

$$F(\phi_1;\phi_1^*,\gamma)=\frac{1}{\pi}\arctan\left(\frac{\phi_1-\phi_1^*}{\gamma}\right)+0.5 \tag{5}$$

and

$$\phi_1^*=\frac{9(S_{33})_1[1-(S_{33})_1]}{-9[(S_{33})_1]^2+15(S_{33})_1+2} \tag{6}$$

where σ_{ii}^c (i = 1 and 3) is the electrical conductivity of the MWCNTs in the i direction, the superscript c represents the thinly coated MWCNTs as surrounded by interface resistivity [19], and r is the outer radius of MWCNTs. ρ_0 is the interfacial resistivity between polymer and MWCNTs and γ is the scale parameter, which related with the probability density function [19].

In addition, the MWCNT shape within the polymer matrix is modeled as a 3D-variable helical spring (Fig. 1) to consider filler morphologies in the viscous PC matrix. The curviness of CNTs has generally been modeled as a sine function or given a bow-shaped appearance by many researchers [21–23]. These curvy shapes could be a good substitute for describing films and two-dimensional (2D) composites; however, in realistic 3D bulk cells, it is not possible to predict the influence of curves in another dimension. In order to develop a rigorous prediction to analyze the morphological effects of nanotubes, the helical aspect ratio (α) of an equivalent inclusion is approximated here as follows [24]:

$$\alpha=\frac{L}{D}=\frac{\varphi}{2\cos\theta} \tag{7}$$

In this equation, where L denotes the equivalent length, D is the spring diameter, φ signifies the polar angle and θ is the spiral angle. The descriptions of the symbols in Eq. (7) are illustrated in detail in Fig. 1.

From Eq. (7), α is fully agglomerated at $\varphi = 0$, while $\varphi \to \infty$ corresponds to a straight CNT. Given that the adopted effective medium theory [19] can consider only two-phase constituents (matrix and filler), the probability concept of the center of gravity (COG) of the polar angle is applied to set the representative value of φ, as follows:

$$\varphi_{cog}=\frac{\int_0^{2\pi}\varphi\cdot[CDF(\varphi_i)-CDF(\varphi_{i-1})]d\varphi}{\int_0^{2\pi}[CDF(\varphi_i)-CDF(\varphi_{i-1})]d\varphi} \tag{8}$$

In Eq. (8), the cumulative distribution function (CDF) can be simplified to a probability density function (PDF), as follows:

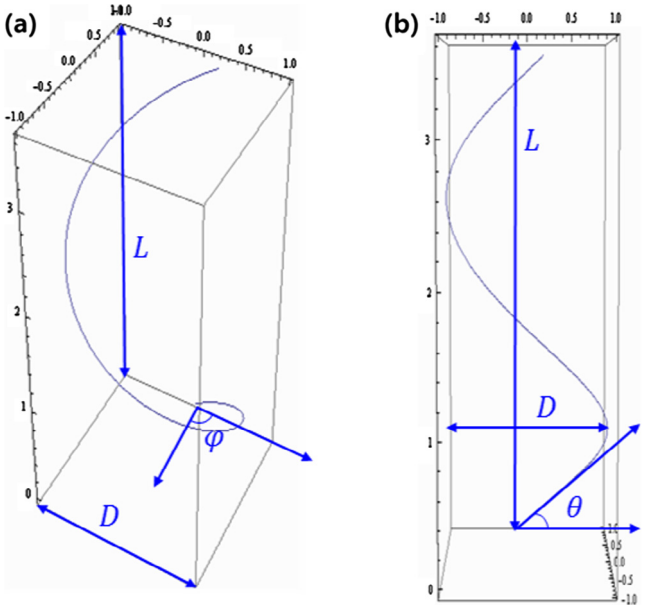

Fig. 1. Illustration in (a) 3D and (b) front view of the present curved MWCNTs: L and D denote the effective length and diameter of the curved MWCNT; φ and θ signify the polar and spiral angle, respectively. The representative value of φ is estimated by the center of gravity (COG) method with a cumulative distribution function, while the representative θ value is determined with the average method, as θ is not affected by φ when the nanotubes are randomly and uniformly distributed in the Cartesian coordinate system. (For interpretation of the references to colour in this figure legend, the reader is referred to the web version of this article.)

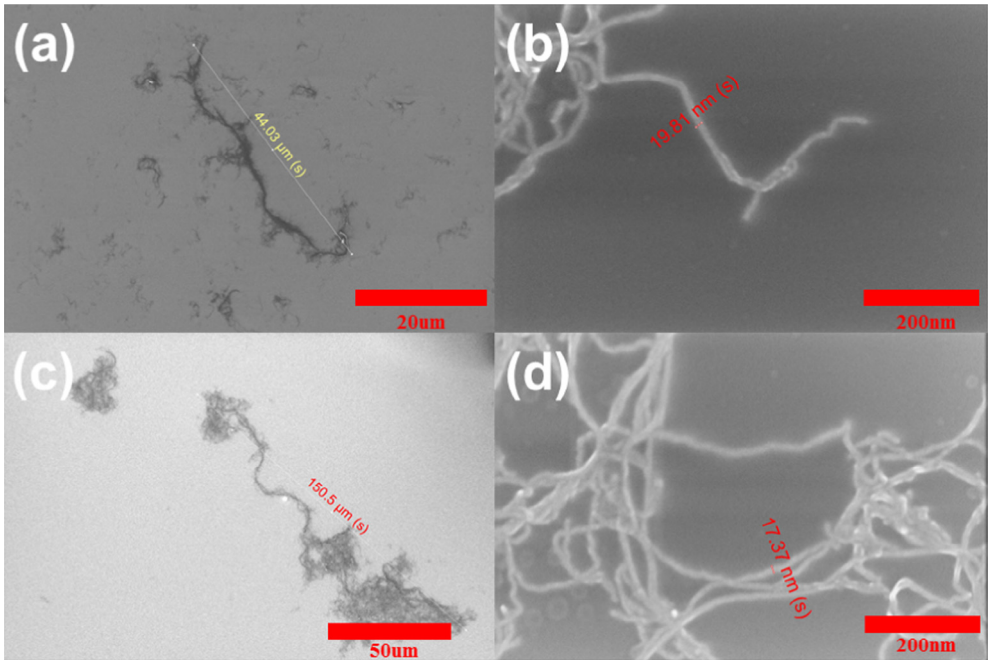

Fig. 2. SEM image analyses of the MWCNTs: the length of the (a) short (30–130 μm) and (b) long (150–250 μm) MWCNTs, and the diameter of the (c) short and (d) long MWCNTs (17–20 nm). (For interpretation of the references to colour in this figure legend, the reader is referred to the web version of this article.)

Table 1
The compositions of the MWCNTs/PC composite samples.

Sample	PC (wt.%)	Short MWCNT (wt.%)	Long MWCNT (wt.%)
S0.5	99.5	0.5	0
S1.0	99.0	1.0	0
S3.0	97.0	3.0	0
S5.0	95.0	5.0	0
S7.0	93.0	7.0	0
S10.0	90.0	10.0	0
L0.5	99.5	0	0.5
L1.0	99.0	0	1.0
L3.0	97.0	0	3.0
L5.0	95.0	0	5.0
L7.0	93.0	0	7.0
L10.0	90.0	0	10.0

$$\varphi_{cog} = \int_0^{2\pi} \varphi \cdot PDF(\varphi_i) d\varphi \tag{9}$$

Hence, the representative degree of the polar angle (φ) can be probabilistically expressed as

$$f(\varphi_{cog}) = \frac{1}{\varphi_{cog} s\sqrt{2\pi}} \exp\left(-\frac{(\ln\ \varphi_{cog} - \mu)^2}{2s^2}\right) \tag{10}$$

where μ is the mean value parameter and s is the standard deviation parameter, which denotes the curviness distribution of the MWCNTs.

When the nanotubes are randomly and uniformly distributed, the spiral angle is not affected by the polar angle because the dispersion direction of the CNTs is considered as the spiral angle in the fixed Cartesian coordinate system in this study. Therefore, with the average method, the representative spiral angle can be simplified as in an earlier study [25]

$$\bar{f}(\theta) = \frac{\int_0^{\frac{\pi}{2}} \sin\theta d\theta}{\pi/2} = \frac{2}{\pi} \tag{11}$$

From the proposed probabilistic model, it is noted that there are four unknown constants (ρ_0, γ, μ and s) for prediction of electrical conductivity of nanocomposites. For a precise prediction of electrical performances of MWCNTs-embedded nanocomposites, the probabilistic parameters should be properly determined; however, the estimation of the optimal parameter set by manually is not guaranteed to find the most reasonable solution. The evolutionary computation method–based genetic algorithm is thus applied in the present study to find the optimal combination of parameters in the proposed model.

The genetic algorithm is one of the most effective approaches that mimic the progress of natural selection by repeating selection, evaluation, reproduction and mutation etc. It can be expressed as [18]:

$$p(x)' = \sum_{y,z \in S} T(x \leftarrow y,z) \frac{w(y)w(z)}{\bar{w}^2} p(y)p(z) \tag{12}$$

and

$$[T(0 \leftarrow y_i, z_j)]_{i,j=1}^{n} \tag{13}$$

where $p(x)$ is the frequency of chromosome x in the population, S is the search scope of chromosomal types and $w(x)$ is the fitness of chromosome x [26]. $T(x \leftarrow y,z)$ means the transmission function and $[T(0 \leftarrow y_i, z_j)]_{i,j=1}^{n}$ is the mixing matrix as a cross-reference [27]. In the present genetic algorithm, the population size and generation number are set to be 100 [26,27]. Note that the chromosome is a set of parameters, representing a solution candidate of the given problem. Hence, the chromosome should be defined in the present study as the interfacial resistivity (ρ_0), scale parameter (γ), curviness mean value (μ), and curviness standard deviation (s). Since the model parameters of the proposed micromechanical modeling are not determined, the optimal set of the unknown parameters (chromosome) are estimated by the genetic algorithm.

3. Experiments

3.1. Materials

The MWCNTs (JC72 and JC142) used here were supplied by Jeio Co., Ltd. (Incheon, Korea). As shown in Fig. 2, they were 30–250 μm

long and with diameters of 17–20 nm, and they had a bulk density of 0.01 g/cc. Linear PC resins (Lupoy PC 1300-03, LG Chemical Co., Gyeonggi-do, Korea) designed for extrusion and injection molding applications were utilized as the matrix of the composites. The Vicat softening point was 151 °C when measured according to ASTM D696 under 50 °C/hr and 50 N load conditions. In addition, the resin density was 1200 kg/m^3 as measured according to ASTM D792 and the melt flow rate was measured as 3 g per 10 min according to ASTM D1238.

3.2. Fabrication of nanocomposites

The MWCNTs and PC resin were prepared such that they would have the respective target contents listed in Table 1; they were mixed at a screw speed of 60 rpm using a HAAKE Rheomix internal mixer (HAAKE™ Rheomix OS Lab Mixers, Thermo Scientific Inc., Marietta, GA, USA) maintained at 260 °C for 30 min, after which the mixture was pelletized. With the produced pellets in a mold, a heating press (D3P-30J, Daheung Science, Incheon, Korea) was used to prepare 2-mm-thick samples 2.5 cm^2 to measure the electrical conductivity. They were thermally compressed to a pressure of 15 MPa for 10 min at 260 °C and then quenched to 30 °C with cooling water.

3.3. Characterization

3.3.1. Morphology

MWCNTs were dispersed for 30 min at a concentration of 0.1 mg per 10 ml of ethanol using an ultrasonic bath (JAC-2010P, Kodo Technical Research Co. Ltd., Gyeonggi-do, Hwaseong, Korea). The dispersed MWCNTs were coated at 3000 rpm for 30 s on a silicon wafer using a spin coater (spin process controller, MIDAS, Daejeon, Korea). The fabricated composites were fractured using liquid nitrogen for sampling, and the prepared samples were surface-coated with platinum for 120 s in a vacuum by a sputter coating machine (Ion Sputter E-1030, Hitachi High Technologies, Tokyo, Japan). The coated MWCNT and composite samples were observed using field-emission scanning electron microscopy

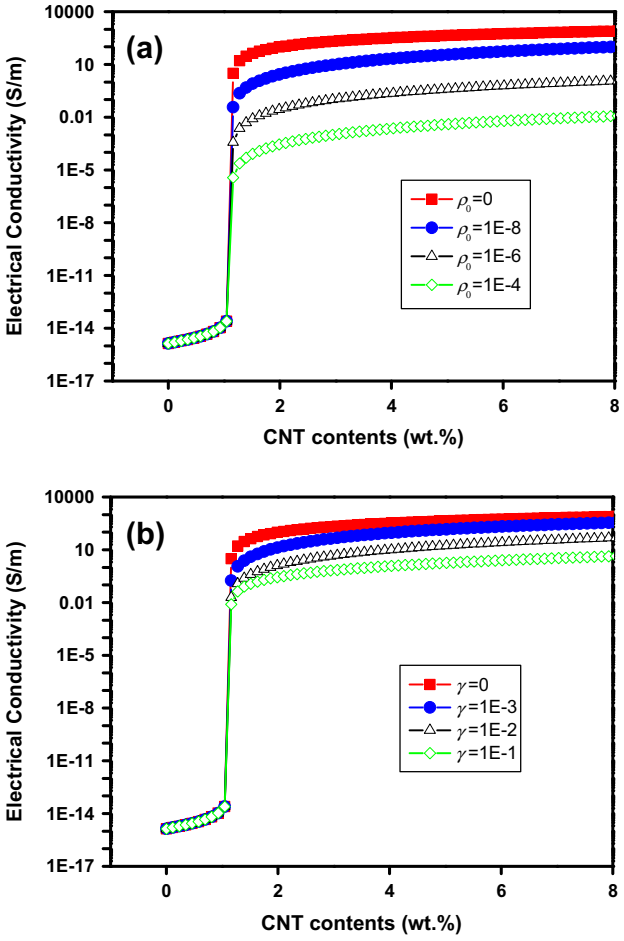

Fig. 4. The present predicted electrical conductivity versus CNT contents with an increase in the (a) interface resistivity and (b) scale parameters. (For interpretation of the references to colour in this figure legend, the reader is referred to the web version of this article.)

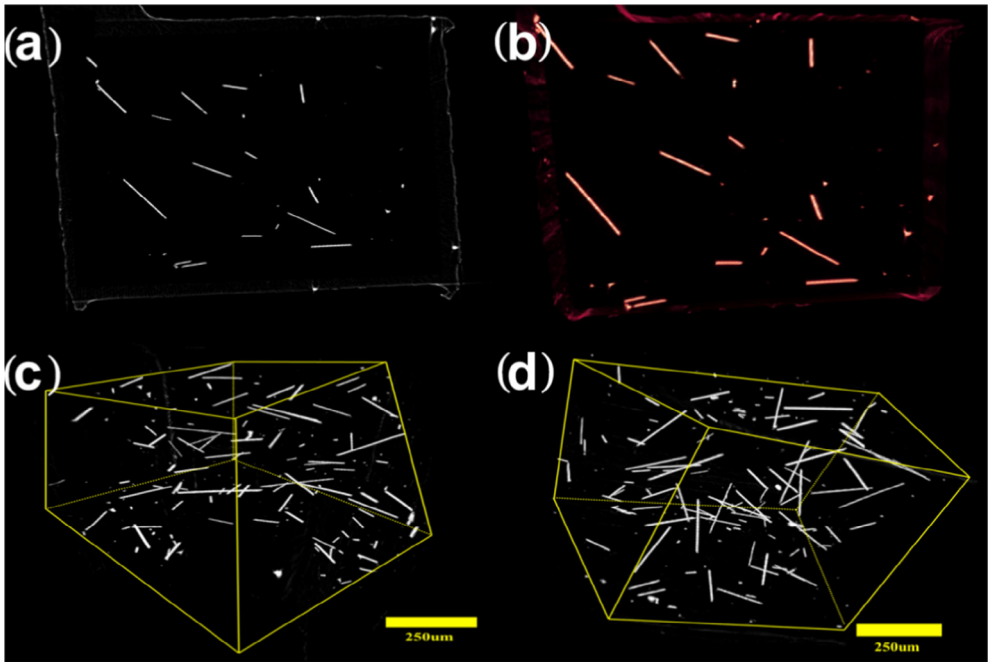

Fig. 3. A description of the micro-CT image processing step: (a) a scanned section image (2000 × 1332 pixels) of composites (long MWCNTs 10 wt.%), (b) a reconstructed image extracted from the initial image data, and (c) and (d) rendered 3D micro-CT images of the entire set of composites at different angles. (For interpretation of the references to colour in this figure legend, the reader is referred to the web version of this article.)

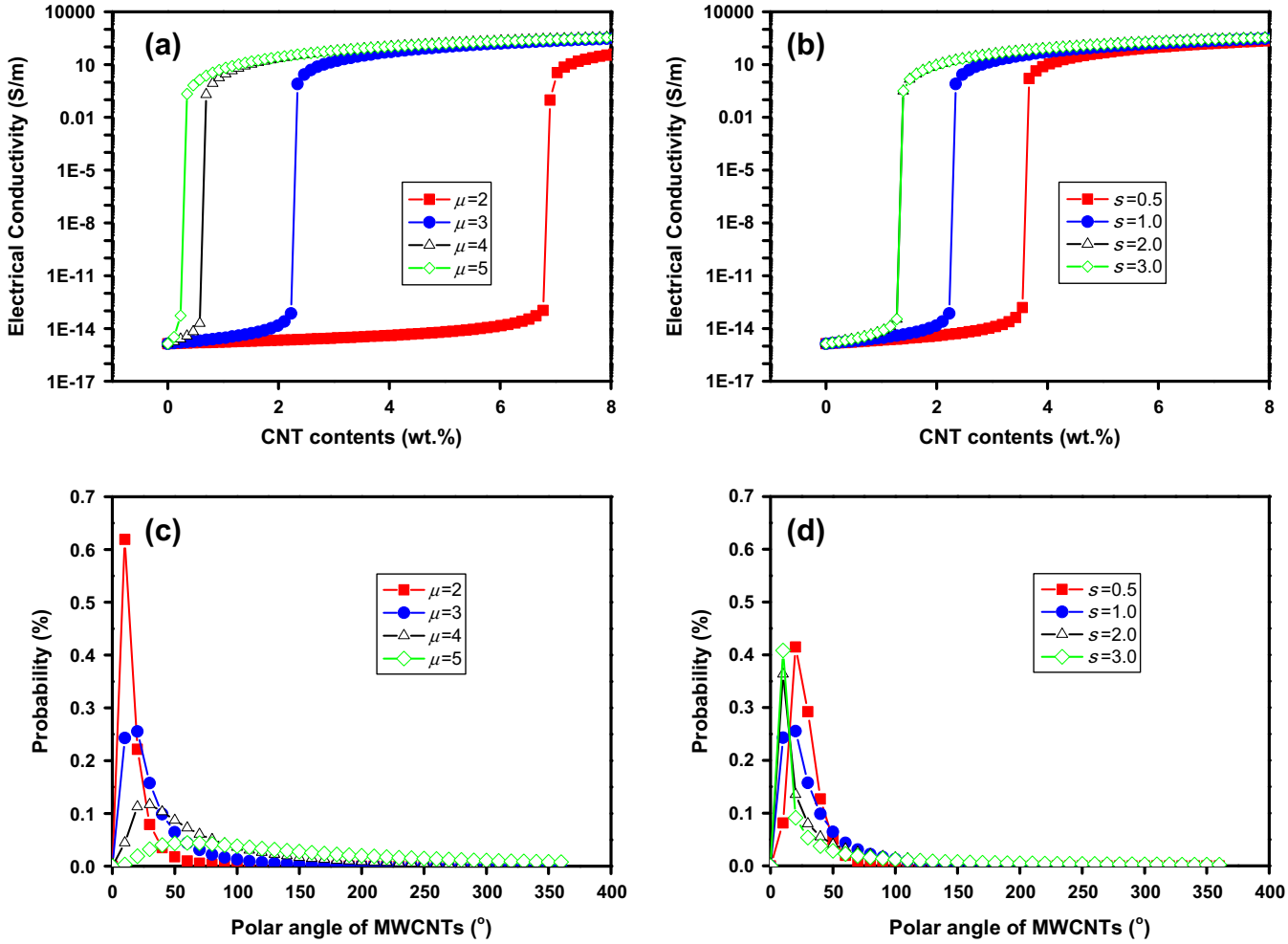

Fig. 5. The results of the parametric analysis: the predicted effective electrical conductivity levels of nanocomposites with varying values of (a) μ and (b) s; the predicted MWCNTs network distribution with respect to (c) μ corresponding to Fig. 3(a) and (d) s corresponding to Fig. 3(b). (For interpretation of the references to colour in this figure legend, the reader is referred to the web version of this article.)

(FE-SEM, Nova NanoSEM 450, FEI Corp., OR, USA) with a voltage of 10 kV applied in a nitrogen vacuum.

3.3.2. Functionality and defect level of MWCNTs

To analyze the functionality of the two types of MWCNTs (short and long), the surfaces of two types of MWCNTs were assessed by Fourier transform infrared spectroscopy (FT-IR, Nicolet iS 10, Thermo Fisher Scientific., USA) with a resolution of 1 cm^{-1} in a wavenumber range of 1000–4000 cm^{-1}. X-ray photoelectron spectroscopy (XPS, AXIS-HSi, Kratos, Kyoto, Japan) with an Mg X-ray source was also utilized with a power of 150 W under a pressure of 1×10^{-8} Torr for a functionality analysis. Moreover, the defect levels of the MWCNTs were measured using a Raman spectroscope (LabRAM HR 800, HORIBA Jobin Yvon, Japan) with a 514 nm Ar-ion laser in the wavenumber range of 1000–3000 cm^{-1} at a magnification of 50.

3.3.3. Tomography

A Micro-CT system (Skyscan 1172, Bruker co, Billerica, MA, USA) was used to measure the dispersion and network structures of the fillers in the composites. The measurements were taken at a size of 2000 × 1332 pixels, and the X-ray source was measured at a voltage of 51 kV and a current of 194 μA under normal pressure. Two-dimensional (2D) images were taken cumulatively in the direction of the sample thickness, as shown in Fig. 3(a), and were reconstructed into 3D images, as shown in Fig. 3(b)–(d). All of the internal structures of the samples for which MWCNTs are randomly dispersed and oriented were then measured in a non-destructive manner.

3.3.4. Electrical conductivity

The effective electrical conductivity of the composites is one of the most critical factors influenced by the MWCNT morphology. In addition, it is emphasized as an important parameter due to influence on industrial applications. The electrical conductivity of the MWCNT/PC composites was therefore measured in the present study using an ultrahigh resistance meter (SM-8220, HIOKI E.E. Corporation, Nagano, Japan) at an applied voltage of 10 V and with the four-probe method according to ASTM D 257 (FPP-RS8, DASOL ENG, Cheongju, Korea).

4. Result and discussions

4.1. Parametric study

Based on the developed probabilistic modeling, the correlations between the model parameter and the effective electrical property of the nanocomposites are numerically investigated. The MWCNT/PC composite is considered in this simulation, with the material properties applied, as follows: L = 30 μm, D = 18 nm,

σ_0 = 1.37E−15 S/m and σ_{33} = 5.1E4 S/m [28]. The value of σ_{11} is relatively low compared to that of σ_{33} in general, and the relationship is assumed to be expressed by $\sigma_{11} = \sigma_{33}$E−3 in the present study.

With the material properties, the electrical conductivity of the MWCNT-reinforced PC composite with various interface resistivities (ρ_0) and scale parameters (γ) is simulated, as shown in Fig. 4. As shown in Fig. 4(a) and (b), the electrical conductivity is generally reduced when the values of ρ_0 and γ increase. However, the parameters ρ_0 and γ are less influential on the percolation threshold that the minimum filler content to lead significant change in the electrical properties of the composites.

Additional parametric studies are carried out to analyze the electrical properties of the composites under various scenarios. The same material constants utilized in the previous tests are applied in the simulations. Fig. 5(a) and (b) shows the predicted electrical conductivity levels of the nanocomposites with various values of μ and s. It is predicted that a higher value of μ and lower value of s lead to an earlier percolation threshold response, and their effects are influential on the overall electrical behavior of the composites [29]. The calculated distribution of MWCNTs corresponding Fig. 5(a) and (b) are also shown in Fig. 5(c) and (d), respectively. The polar angle of MWCNTs is varying as the response to μ and s variations, indicating that the μ and s must be accurately estimated for a more realistic prediction.

In order to evaluate the sensitivity of the present model to the MWCNT length, an additional parametric analysis is carried out, as shown in Fig. 6. Considering the findings in earlier work [30–32], various lengths of MWCNT for the simulation were considered here. The diameter of the MWCNTs is assumed to be D = 18 nm. Fig. 6 shows that the MWCNT length has a considerable influence on the percolation threshold and the overall electrical performance of the nanocomposites. More rapid and better electrical properties are calculated with a longer filler length. It appeared that the length of the MWCNT filler material does not affect the percolation threshold before the certain filler content point; however, the effective electrical performance level of the composites is improved as the MWCNT length increases. However, it should be noted that these predicted results can be established by assuming the same morphological properties and agglomeration degrees of MWCNTs, irrespective of the filler length.

4.2. Experimentally determined electrical conductivity

The electrical conductivity of polymer composites filled with carbon fillers is known to depend on the morphology of the fillers, the dispersion of the fillers, and the defect level of the fillers which is related to their electrical conductivity. To investigate the effect the MWCNT length on the electrical conductivity of polymer composites, the effects of the physical parameters other than the MWCNT length on the electrical conductivity should be minimized. SEM images of the length and diameter of both the short and long MWCNTs are shown in Fig. 2. From the analyses, the representative length and diameter of the MWCNTs, which are the important physical features in the present simulation study, can be approximated. Similar diameters of the short and long MWCNTs were found, ranging from 17 to 20 nm, though different lengths were observed.

Table 2
Electrical conductivity of the fabricated composites with different filler types and contents.

Filler content (wt.%)	Electrical conductivity (S/m)	
	Long MWCNT	Short MWCNT
0.0	$1.37E^{-15}$	
0.5	$2.92E^{-4}$	$2.12E^{-4}$
1.0	$5.13E^{-4}$	$3.05E^{-4}$
3.0	$3.20E^{-2}$	$7.92E^{-3}$
5.0	$1.90E^{0}$	$3.49E^{-2}$
7.0	$1.70E^{2}$	$1.70E^{2}$
10.0	$2.49E^{2}$	$9.74E^{1}$

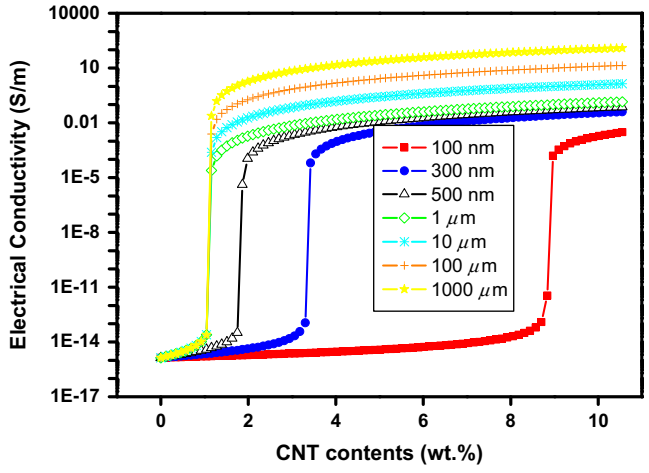

Fig. 6. The present predicted electrical conductivity of MWCNT/PC composites with various lengths of MWCNTs. (For interpretation of the references to colour in this figure legend, the reader is referred to the web version of this article.)

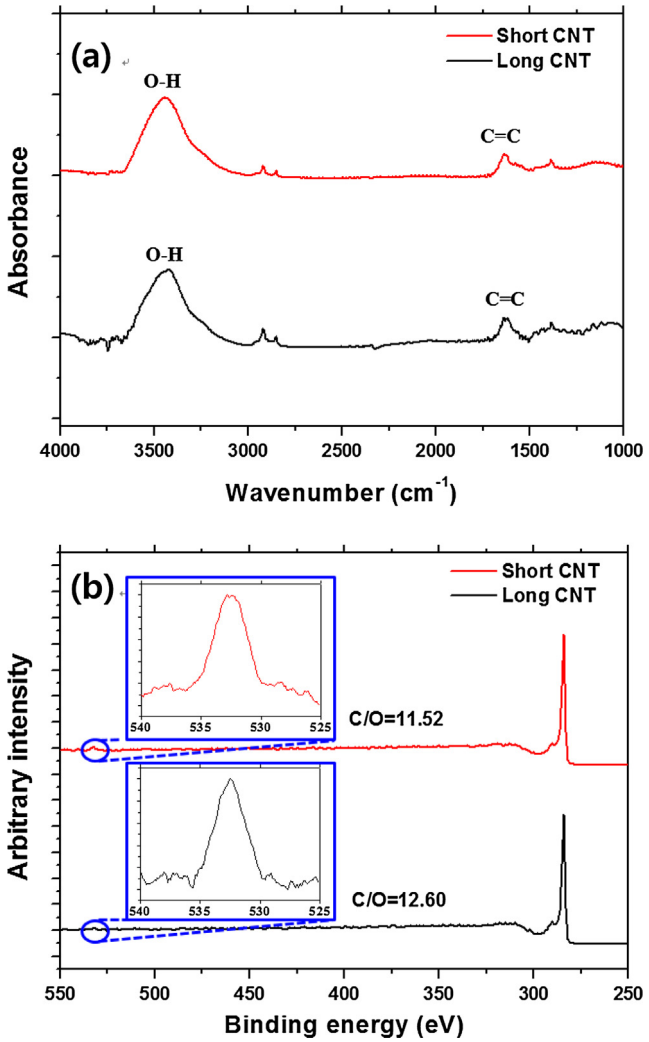

Fig. 7. The experimental analysis results from (a) FT-IR and (b) XPS. (For interpretation of the references to colour in this figure legend, the reader is referred to the web version of this article.)

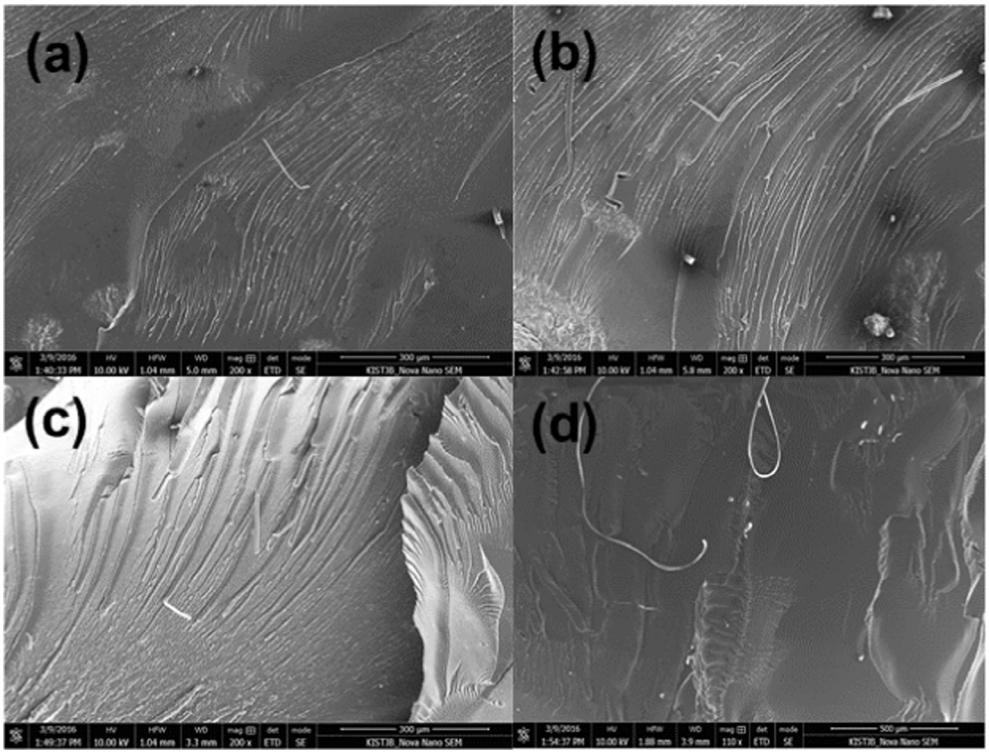

Fig. 8. SEM images of the fracture surfaces of composites filled with (a) 5 wt.% short MWCNTs, (b) 10 wt.% short MWCNTs, (c) 5 wt.% long MWCNTs and (d) 10 wt.% long MWCNTs.

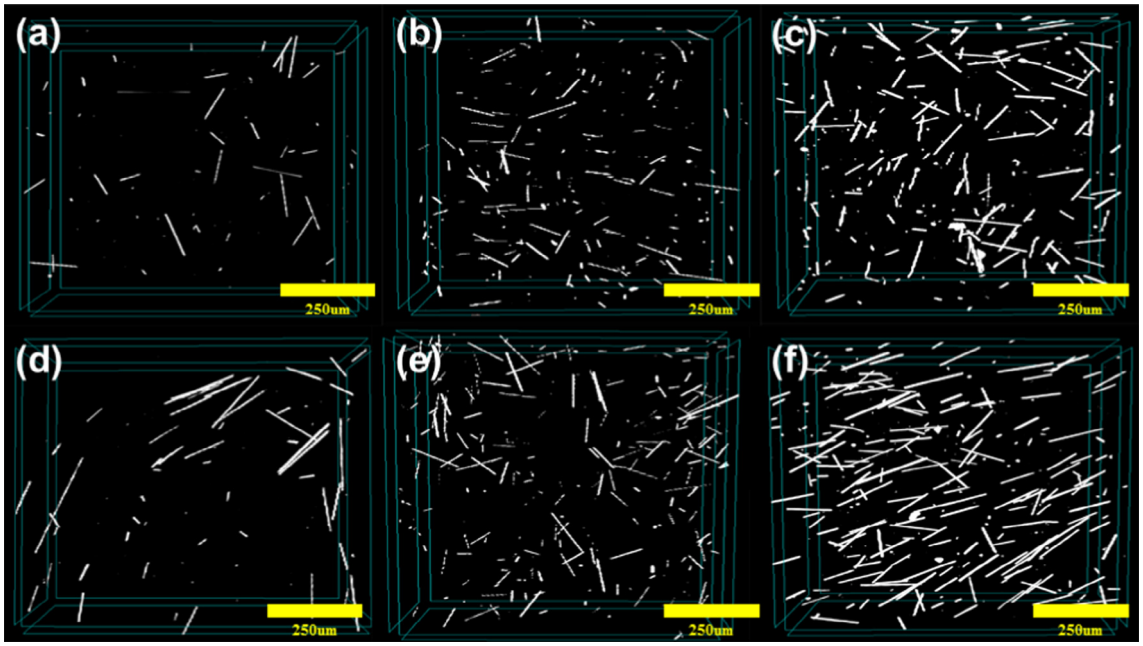

Fig. 9. Micro-CT images of composites filled with (a) 1 wt.% short MWCNTs, (b) 5 wt.% short MWCNTs, (c) 10 wt.% short MWCNTs, (d) 1 wt.% long MWCNTs, (e) 5 wt.% long MWCNTs and (f) 10 wt.% long MWCNTs. (For interpretation of the references to colour in this figure legend, the reader is referred to the web version of this article.)

The electrical conductivity levels of the fabricated composites with various contents of MWCNTs are listed in Table 2. This table demonstrates that the percolation thresholds of both samples occurred at a similar point (0.5 wt.%) regardless of the CNT length. The overall electrical trends of the composites are also not significantly different; however, the samples containing long MWCNTs showed slightly better performance. These results are presumed to be due to the weakened tunneling effect of the short MWCNTs [33], resulting in a proportional decrease in the electrical conductivity of the nanocomposites. This indicates that the longer MWCNT filler may offer improved effective electrical properties of MWCNT-embedded PC composites past the percolation threshold.

The FT-IR and XPS results of the MWCNTs are shown in Fig. 7 for a quantitative evaluation of the effects of the structural and chemical characteristics of the MWCNTs, as these factors significantly

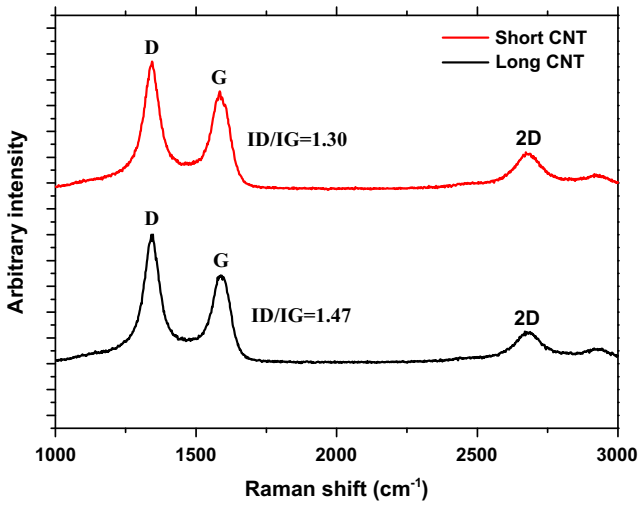

Fig. 10. Raman spectroscopy results of nanocomposites containing short and long MWCNTs. (For interpretation of the references to colour in this figure legend, the reader is referred to the web version of this article.)

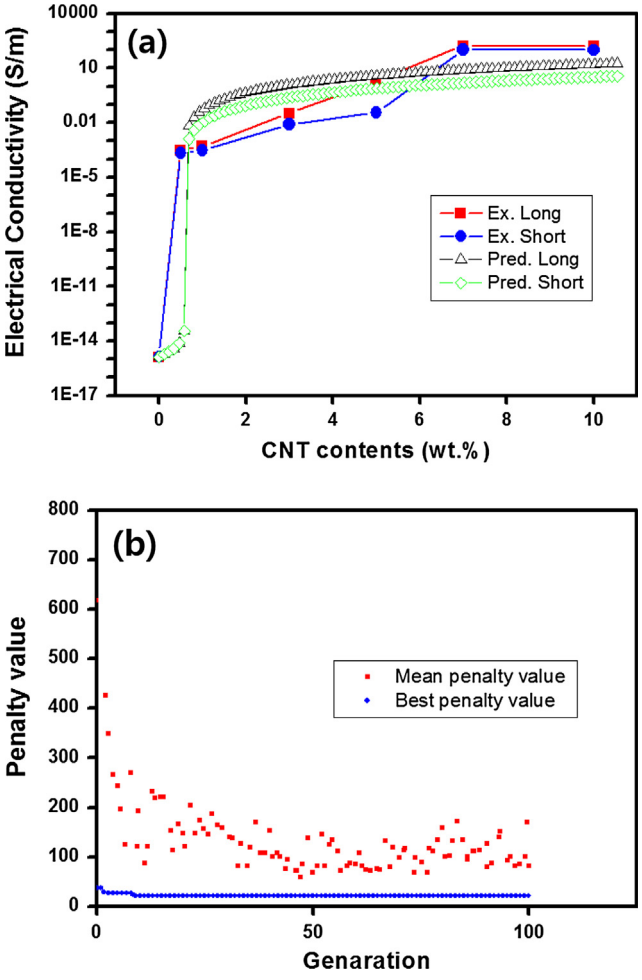

Fig. 11. (a) Comparison between the present predictions and experimental data for the effective electrical conductivity of the composites. Long (≈150 μm) and short (≈30 μm) lengths of the MWCNTs embedded into the PC matrix; (b) the corresponding mean and best penalty values calculated by the genetic algorithm. (For interpretation of the references to colour in this figure legend, the reader is referred to the web version of this article.)

influence the interfacial and dispersion characteristics. As shown in Fig. 7(a), both the short and long types of MWCNTs exhibited O—H bond peaks at 3440 cm^{-1} and C=C bond peaks at 1655 cm^{-1} with similar intensities in the FT-IR results. In addition, the similar C/O ratios and intensity were confirmed by XPS measurements as shown Fig. 7(b). From the results, the surface functionality of the short and long MWCNTs did not differ significantly, indicating that the effect of the interfacial properties on dispersion of the MWCNTs was thought to have been minimized.

Figs. 8 and 9 show the fracture-surface morphology and 3D micro-CT images of the composites with respect to the weight fractions of the short and long MWCNT fillers in the composites. Herein, the short and long MWCNTs represent the length of 30–130 and 150–250 μm for MWCNTs, respectively. From the SEM image of the composite fracture surface, it was difficult to determine the degree of the MWCNT filler dispersion accurately, whereas in the X-ray micro-CT image, an excellent filler dispersion was observed regardless of the weight fraction up to 7 wt.%. This indicates that a non-destructive 3D analysis technique such as X-ray micro-CT can be an adequate method with which to assess the dispersion of MWCNT fillers in composites. Furthermore, it was confirmed from the findings that the proposed method for the fabrication of composites can achieve a uniform dispersion of MWCNT fillers.

It was noted in the Raman spectroscopy results, shown in Fig. 10, that D and G peaks appeared at 1339 and 1568 cm^{-1}. The D peak is correlated with disorder caused by a double-resonance Raman scattering process from a non-zero center phonon mode in disordered or amorphous carbon atoms. The G peak arises from the in-plane tangential stretching of carbon-carbon bonds in a graphene sheet [34–38]. Hence, by estimating the intensity ratio of the D and G peaks (ID/IG ratio), the defect level of each type of MWCNT can be evaluated [35–37]. From the ID/IG ratio results of the short and long MWCNTs (1.30 and 1.47), the long MWCNTs are more defective than the short nanotubes. Based on the non-proportional relationship between the ID/IG ratio and the experimentally measured electrical conductivity of the composites as listed in Table 2, the defect level of MWNCTs was one of the minor physical parameters used to determine the electrical conductivity in the employed materials and processing system.

4.3. Comparisons between theoretical and experimental results

The comparisons between the present predictions based on the proposed probabilistic computational model and the experimentally measured electrical conductivity of PC composites containing different lengths of MWCNTs are presented in (a). The aforementioned material parameters are applied to the model, including the different lengths of the MWCNTs (30 μm for short and 150 μm for long MWCNTs). For genetic algorithm, the initial value and the range of each parameter need to be defined as an input data. The initial values of parameters ρ_0, γ, μ and s are assumed to be 0 for all parameters, and the ranges of each parameter are: ρ_0 = 0–1E−4; γ = 0–0.1; μ = 0–5; s = 0–3 based on the numerical simualtions.

The ideal solution for the prediction based on the proposed modeling is then automatically calculated. The estimated model parameters by genetic algorithm are: ρ_0 = 5.82E−7, γ = 4.15E−3, μ = 5.3, s = 3.1, respectively. The same parameters, except for the CNT lengths, are applied in the comparisons to verify the model, and good agreement between the predictions and test results can be observed in Fig. 11(a). As shown in Fig. 11(a), the effect of MWCNT length does not significantly affect to the electrical properties of nanocomposites. However, the main purpose of the comparison is to highlight the applicability of the proposed model, demonstrating the predictive capability on the percolation threshold and electrical conductivity of nanocomposites. Overall, the

present predictions match well with the experimental results under the laboratory conditions, showing the potential of the developed model considering MWCNT morphology and interface effects. In addition, it is noted that the predictions of experimental comparisons in Fig. 11 and numerical simulations in Fig. 6 are similar with the 30–250 μm range of MWCNT length. The mean and best penalty values for the calculation are shown in Fig. 11(b) corresponding to Fig. 11(a). The penalty value in genetic algorithm represents the calculated results of objective function, which penalize infeasible solutions to find an optimal solution. In Fig. 11(b), the mean penalty value denotes the average penalty value over the entire current population, while the best penalty value means the optimal solution within the current generation [39]. More detailed description of the penalty value in genetic algorithm can be found in [40].

5. Conclusions

In the present study, we have investigated the correlations between the MWCNT properties and the effective electrical properties of PC matrix composites containing 3D randomly oriented MWCNTs. A theoretical study is carried out, and the electrical behaviors of nanocomposites under various conditions are predicted and evaluated. MWCNTs with different lengths were also intentionally utilized in an experimental study to analyze the effects of their morphology in a PC matrix. The observations and findings from the study are summarized below.

(1) A probabilistic model is newly proposed. The model parameters of the present theoretical framework are estimated by the evolutionary computation method–based genetic algorithm.
(2) The morphological characteristics of MWCNTs and composites are analyzed by various approaches, including micro-CT, FT-IR, XPS, Raman, and SEM analyses.
(3) The composites in the present work showed excellent filler dispersions and electrical properties with the proposed fabrication method, which is simple and has a low manufacturing cost.
(4) It is calculated from the numerical simulations that the interface-related parameters (ρ_0 and γ) are influential on the maximum electrical conductivity of composites, while the MWCNTs network-related parameters (μ and s) affect the percolation threshold.
(5) It is calculated from the proposed model that the overall electrical performance of the composites can be improved as the CNT length increases. However, the length of filler may not affect the percolation threshold when the content is too small.
(6) To verify the proposed model, same parameters with different material constituents are considered in the experimental comparisons. In overall, good agreement between the predictions and test results can be observed.

Acknowledgements

This study was supported by the Korea Institute of Science and Technology (KIST) Institutional Program and the Technological innovation R&D program of SMBA [S2394169]. It was also supported by Nano·Material Technology Development Program through the National Research Foundation of Korea (NRF) funded by the Ministry of Science, ICT and Future Planning (2016M3A7B4027695).

References

[1] Al-Saleh MH, Sundararaj U. Review of the mechanical properties of carbon nanofiber/polymer composites. Compos Part A Appl Sci Manuf 2011;42(12):2126–42.
[2] Yang B, Souri H, Kim S, Ryu S, Lee H. An analytical model to predict curvature effects of the carbon nanotube on the overall behavior of nanocomposites. J Appl Phys 2014;116(3):033511.
[3] Wang X, Jiang Q, Xu W, Cai W, Inoue Y, Zhu Y. Effect of carbon nanotube length on thermal, electrical and mechanical properties of CNT/bismaleimide composites. Carbon 2013;53:145–52.
[4] Akhter T, Mun SC, Saeed S, Park OO, Siddiqi HM. Enhancing the dielectric properties of highly compatible new polyimide/γ-ray irradiated MWCNT nanocomposites. RSC Adv 2015;5(87):71183–9.
[5] Shi X, Wang SH, Shen M, Antwerp ME, Chen X, Li C, et al. Multifunctional dendrimer-modified multiwalled carbon nanotubes: synthesis, characterization, and in vitro cancer cell targeting and imaging. Biomacromolecules 2009;10(7):1744–50.
[6] Oh Y, Islam MF. Preformed nanoporous carbon nanotube scaffold-based multifunctional polymer composites. ACS Nano 2015;9(4):4103–10.
[7] Hudgin D, Bendler T. Handbook of polycarbonate science and technology. New York: Marcel Dekker Inc.; 2000.
[8] Maiti S, Shrivastava N, Suin S, Khatua B. A strategy for achieving low percolation and high electrical conductivity in melt-blended polycarbonate (PC)/multiwall carbon nanotube (MWCNT) nanocomposites: electrical and thermo-mechanical properties. Exp Polym Lett 2013;7(6):505–18.
[9] Zhou J, Lubineau G. Improving electrical conductivity in polycarbonate nanocomposites using highly conductive PEDOT/PSS coated MWCNTs. ACS Appl Mater Interfaces 2013;5(13):6189–200.
[10] Rafiee R, Moghadam RM. On the modeling of carbon nanotubes: a critical review. Compos Part B-Eng 2014;56:435–49.
[11] Liew KM, Lei ZX, Zhang LW. Mechanical analysis of functionally graded carbon nanotube reinforced composites: a review. Compos Struct 2015;120:90–7.
[12] Klein ML, Shinoda W. Large-scale molecular dynamics simulations of self-assembling systems. Science 2008;321(5890):798–800.
[13] Gibson RF. A review of recent research on mechanics of multifunctional composite materials and structures. Compos Struct 2010;92(12):2793–810.
[14] Lubineau G, Nouri H, Roger F. On micro–meso relations homogenizing electrical properties of transversely cracked laminated composites. Compos Struct 2013;105:66–74.
[15] Seidel GD, Lagoudas DC. A micromechanics model for the electrical conductivity of nanotube-polymer nanocomposites. J Compos Mater 2009;43(9):917–41.
[16] Deng F, Zheng QS. An analytical model of effective electrical conductivity of carbon nanotube composites. Appl Phys Lett 2008;92(7):071902.
[17] Pyo S, Lee H. An elastoplastic damage model for metal matrix composites considering progressive imperfect interface under transverse loading. Int J Plast 2010;26(1):25–41.
[18] Deb K, Pratap A, Agarwal S, Meyarivan T. A fast and elitist multiobjective genetic algorithm: NSGA-II. IEEE Trans Evol Comput 2002;6(2):182–97.
[19] Wang Y, Weng GJ, Meguid SA, Hamouda AM. A continuum model with a percolation threshold and tunneling-assisted interfacial conductivity for carbon nanotube-based nanocomposites. J Appl Phys 2014;115(19):193706.
[20] Hashemi R, Weng GJ. A theoretical treatment of graphene nanocomposites with percolation threshold, tunneling-assisted conductivity and microcapacitor effect in AC and DC electrical settings. Carbon 2016;96:474–90.
[21] Abdin Y, Jain A, Verpoest I, Lomov S. Mean-field based micro-mechanical modelling of short wavy fiber reinforced composites. Compos Part A Appl Sci Manuf 2016. http://dx.doi.org/10.1016/j.compositesa.2016.03.022 [in press].
[22] Tsai C-h, Zhang C, Jack DA, Liang R, Wang B. The effect of inclusion waviness and waviness distribution on elastic properties of fiber-reinforced composites. Compos Part B-Eng 2011;42(1):62–70.
[23] Yazdchi K, Salehi M. The effects of CNT waviness on interfacial stress transfer characteristics of CNT/polymer composites. Compos Part A Appl Sci Manuf 2011;42(10):1301–9.
[24] Shi D-L, Feng X-Q, Huang YY, Hwang K-C, Gao H. The effect of nanotube waviness and agglomeration on the elastic property of carbon nanotube-reinforced composites. J Eng Mater Technol 2004;126(3):250–7.
[25] Yang B, Cho K, Kim G, Lee H. Effect of CNT agglomeration on the electrical conductivity and percolation threshold of nanocomposites: a micromechanics-based approach. Comput Model Eng Sci 2014;103(5):343–65.
[26] Altenberg L. The schema theorem and Price's theorem. Found Genetic Algor 1995;3:23–49.
[27] Schmitt LM. Theory of genetic algorithms. Theoret Comput Sci 2001;259(1):1–61.
[28] Kim SY, Noh YJ, Yu J. Prediction and experimental validation of electrical percolation by applying a modified micromechanics model considering multiple heterogeneous inclusions. Compos Sci Technol 2015;106:156–62.
[29] Yang B, Shin H, Kim H, Lee H. Strain rate and adhesive energy dependent viscoplastic damage modeling for nanoparticulate composites: molecular dynamics and micromechanical simulations. Appl Phys Lett 2014;104(10):101901.

[30] Coleman JN, Khan U, Blau WJ, Gun'ko YK. Small but strong: a review of the mechanical properties of carbon nanotube–polymer composites. Carbon 2006;44(9):1624–52.
[31] Ma P-C, Siddiqui NA, Marom G, Kim J-K. Dispersion and functionalization of carbon nanotubes for polymer-based nanocomposites: a review. Compos Part A Appl Sci Manuf 2010;41(10):1345–67.
[32] Thostenson ET, Ren Z, Chou T-W. Advances in the science and technology of carbon nanotubes and their composites: a review. Compos Sci Technol 2001;61(13):1899–912.
[33] Li C, Thostenson ET, Chou T-W. Dominant role of tunneling resistance in the electrical conductivity of carbon nanotube–based composites. Appl Phys Lett 2007;91(22):223114.
[34] Kim HS, Bae HS, Yu J, Kim SY. Thermal conductivity of polymer composites with the geometrical characteristics of graphene nanoplatelets. Sci Rep 2016;6:26825.
[35] Noh YJ, Joh H-I, Yu J, Hwang SH, Lee S, Lee CH, et al. Ultra-high dispersion of graphene in polymer composite via solvent free fabrication and functionalization. Sci Rep 2015;5:9141.
[36] Kim HS, Jang J-U, Yu J, Kim SY. Thermal conductivity of polymer composites based on the length of multi-walled carbon nanotubes. Compos Part B-Eng 2015;79:505–12.
[37] Noh YJ, Pak SY, Hwang SH, Hwang JY, Kim SY, Youn JR. Enhanced dispersion for electrical percolation behavior of multi-walled carbon nanotubes in polymer nanocomposites using simple powder mixing and in situ polymerization with surface treatment of the fillers. Compos Sci Technol 2013;89:29–37.
[38] Pak SY, Kim HM, Kim SY, Youn JR. Synergistic improvement of thermal conductivity of thermoplastic composites with mixed boron nitride and multi-walled carbon nanotube fillers. Carbon 2012;50(13):4830–8.
[39] Yeniay ö. Penalty function methods for constrained optimization with genetic algorithms. Math Comput Appl 2005;10:45–56.
[40] Bäck T, Fogel DB, Michalewicz Z. Handbook of evolutionary computation. IOP Publishing Ltd and Oxford University Press; 1997. B1.